Combust. Sci. and Tech., 1991, Vol. 80, pp. 1–21
Photocopying permitted by license only

Simultaneous Multiline Emission Absorption Measurements in Optically Thick Turbulent Flames

Y. R. SIVATHANU and J. P. GORE[1] *Department of Mechanical Engineering, The University of Maryland, College Park and Baltimore County, College Park, MD 20742, Baltimore County, Baltimore, MD 21228*

(*Received February 22, 1991; in final form May 6, 1991*)

Abstract—Simultaneous transient emission/absorption measurements at five wavelengths in strongly radiating, optically thick, turbulent diffusion flames burning acetylene in air were completed. The data were processed to obtain CO_2 mole fractions, temperatures and soot volume fractions spatially resolved to the estimated local integral length scale of mixture fraction fluctuations. Temperatures and soot volume fractions based on emission intensities showed strong negative correlation due to radiative cooling effects. Probability density functions of soot volume fractions conditioned on CO_2 mole fractions showed similarities with position. However, probable effects of negligible diffusivity of soot particles were observed. Probability density functions of soot volume fractions conditioned on both CO_2 concentrations and temperature illustrate the important role of radiative heat transfer in determining the flame structure. A multivariate stochastic analysis resulted in good predictions of radiation intensities.

Key words: Turbulent combustion, radiation, emission/absorption measurements

NOMENCLATURE

c	speed of light
d	burner diameter
f_{va}	absorption soot volume faction
f_{ve}	emission soot volume fraction
F_i	Transmittance for optical filters
h	Planck's constant
i	unit imaginary number $\sqrt{-1}$
I, E	monochromatic radiation intensity
k	imaginary part of the complex refractive index of soot
K_E	molecular line constant
k_B	Boltzmann's constant
K_i	spectral absorption coefficient
L	fixed probe distance
m	fuel mass flow rate
n	real part of the complex refractive index of soot
Q	heat release rate
Re	Reynolds number
r	radial distance from flame axis
T	temperature
t	time
x	axial distance from the burner exit

[1] Present address: School of Mechanical Engineering, Purdue University, West Lafayette, IN 47907.

X mole fraction of gas species
X^* optical depth in the weak line limit
X_R radiative heat loss fraction
Y combined Doppler and collision broadened line width
λ wavelength
Φ coefficient in stochastic simulations, also equivalence ratio
τ transmittance of soot particles and gaseous species

Subscripts

a absorption
b blackbody
CO_2 for carbon dioxide
e emission
s for soot
T temperature
λ monochromatic quantity at λ

Superscripts

′ fluctuating quantity, RMS with an overbar
o original quantity

INTRODUCTION

This article describes the first simultaneous, transient five-wavelength emission/absorption measurements of soot volume fractions, temperature and CO_2 concentrations in turbulent diffusion flames spatially resolved to the estimated local integral length scale of mixture fraction fluctuations. A 6 mm diameter × 6 mm long measurement volume was adequate for this purpose. Acetylene/air diffusion flames were selected due to their high sooting tendency and large radiative heat loss. These flames are also of interest due to the attention they have received in the literature (Magnussen, 1975; Becker and Liang, 1983; Kent and Bastin, 1984; Gore and Faeth, 1988; Gore *et al.*, 1990; Sivathanu, 1990; Sivathanu and Gore, 1990; and Sivathanu *et al.*, 1990, 1991). The objectives of the present work were: (1) to obtain *in situ* measurements of all structure properties that are relevant to radiative heat transfer; and (2) to determine if spatially independent multivariate simulations in conjunction with the above measurements can treat turbulence radiation interactions in strongly radiating diffusion flames.

The radiative heat fluxes from acetylene/air flames are dominated by continuum radiation from soot particles and the CO_2 band at 4300 nm (Gore and Faeth, 1988). For temperatures of interest in practical flames, the absorption cross section of soot particles depends only on their volume fraction (Tien and Lee, 1982). The absorption cross section of CO_2 depends on its mole fraction, the mole fraction of species that cause collision broadening and the local temperature. For atmospheric pressure flames, effects of inaccuracies in estimates of collision broadening on those of radiation intensity are relatively small. Since N_2 forms bulk of the remaining species for most conditions of interest, collision broadening can be estimated using cross sections of N_2. The effectiveness of this approximation was experimentally verified in the present study. Thus, knowledge of local instantaneous soot volume fractions, CO_2 concentrations and temperatures is adequate for the calculation of radiative heat flux. In the present work, these

three quantities were measured *in situ* removing uncertainties characteristic of past studies (Gore and Faeth, 1988; Gore *et al.*, 1990; Sivathanu, 1990; and Sivathanu *et al.*, 1990).

As summarized by Sivathanu *et al.* (1991), the uncertainties in past studies of luminous flame radiation are associated with: (1) turbulence models, (2) approximate state relationships for soot volume fractions, and (3) approximate models for temperatures. Gore and Faeth (1988) used a turbulence model for calculating mixing properties of acetylene/air jet flames. The soot volume fractions and temperatures were uniquely related to the local mixture fraction (fraction of elemental mass that originated in the fuel stream). Unfortunately, measurements showed that soot volume fractions in laminar flames are not uniquely related to mixture fractions and evaluation of the concept for turbulent flames has not been possible. Several investigators have also found that temperatures in strongly radiating jet flames are not uniquely related to mixture fraction but depend on residence time for radiative cooling (Gore *et al.*, 1990; Sivathanu *et al.*, 1991; and Sivathanu and Gore, 1990).

In subsequent work (Gore *et al.*, 1990), the effects of residence time on radiative cooling were treated by conducting coupled structure-radiation calculations. However, uncertainties of the turbulence model, the state relationships for soot volume fractions and the neglect of joint statistics of mixture fraction and enthalpy prevented these calculations from being definitive.

In order to avoid the uncertainties associated with the soot state relationships and the turbulence model, Sivathanu *et al.* (1990) and Sivathanu (1990) used two point *in situ* measurements of soot volume fractions in gaseous pool flames based on absorption of a laser beam. The temperatures were prescribed using an approximate two level (double delta function probability density function-PDF) model (Sivathanu, 1990). Relatively low upper level temperatures (1450 K) were required to obtain satisfactory predictions of radiation intensity for propylene (Sivathanu *et al.*, 1990). However, predictions of radiation intensities for the acetylene flames were not satisfactory with 1350 K as the upper level temperature (Sivathanu, 1990).

Sivathanu *et al.* (1991) found the reason for the above discrepancy. They observed that bulk of the soot measured by the laser absorption probe (termed absorption soot) is relatively cold and does not contribute significantly to the emission of radiation. The temperatures measured by the two wavelength technique are close to the peak values in the probe volume. Based on measurements of emission intensity, Sivathanu *et al.* (1991) estimated the volume fraction of the soot (termed emission soot) that contributed to the radiation intensity. The use of emission soot volume fractions in conjunction with *in situ* measurements of temperature yielded very good predictions of mean and RMS radiation intensities at 900 and 1000 nm. Recently, intensity at 2300 nm and probably density functions and power spectral densities of spectral radiation intensity fluctuations were also predicted reasonably well (Sivathanu and Gore, 1990).

The present study was designed to extend the work of Sivathanu *et al.* (1991) to include measurements of mole fractions of CO_2 and measurements and predictions of spectral radiation intensities from CO_2 + soot at 4500 nm and from soot at 4000 nm. Specific new contributions of this extension are: (1) all the spectral regions relevant to significant radiative heat transfer were treated by including the 4500 nm band of CO_2 in addition to continuum radiation from soot; and (2) a relatively complete description of scalar properties in the flames, resolved to the estimated integral length scale of mixture fraction, was obtained in conjunction with the laminar flamelet approximation.

The article begins with a description of the experimental methods including a discussion of the length scales resolved by the present technique. The multivariate analysis of spectral radiation intensity is then summarized. Mean and RMS scalar measurements of temperature, soot volume fractions and CO_2 mole fractions are then presented.

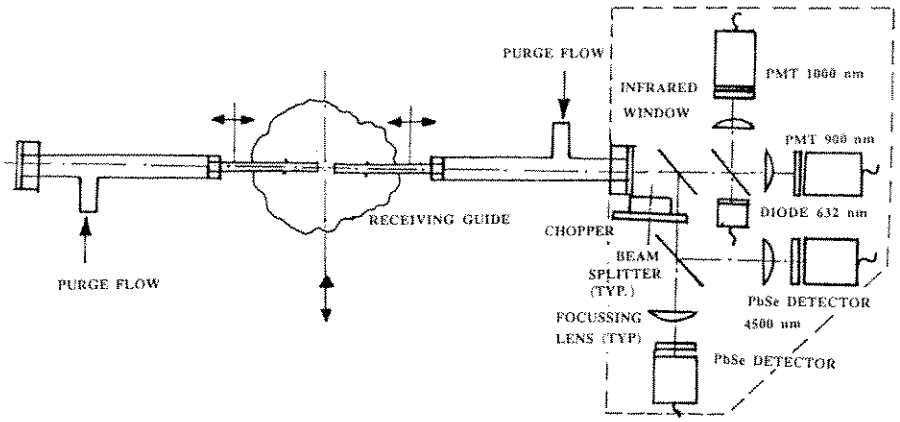

FIGURE 1 A sketch of the 5 line emission absorption probe.

Next, conditional probability density functions are used to study the transient data. Finally, predictions of spectral radiation intensity at 4000 nm and 4500 nm based on a multivariate stochastic model are evaluated using new measurements.

EXPERIMENTAL METHODS

Apparatus

The present burner was identical to the one used by Gore *et al.* (1990) and Sivathanu *et al.* (1991). Fuel was injected vertically upward through a 6 mm diameter 250 mm long uncooled stainless steel tube. The burner can be traversed 400 mm in the vertical direction and 400 mm in the horizontal direction for mapping the entire flame with fixed optics. The burner and the traverses were enclosed in a screened cage ($1 \times 1 \times 2$ m high) to protect the flames from ambient disturbances. For the present operating conditions, the flames attached naturally at the tube exit.

Emission/Absorption Measurements of T, f_{ve}, f_{va} and X_{CO_2}

A five-line optical probe consisting of laser extinction at 632 nm, two wavelength emission pyrometry (900 and 1000 nm) and emission spectroscopy (4000 and 4500 nm) for CO_2 concentrations was used. Measurements of emission intensity of soot at 4000 nm were used to correct the emission signal at 4500 nm for soot interference. The CO_2 mole fractions were inferred from the emission intensity using tables generated from the Goody statistical band model described by Ludwig *et al.* (1973). Soot volume fractions were inferred from both extinction (termed absorption soot) and emission (termed emission soot) measurements. The temperatures were inferred from the emission measurements at 900 nm and 1000 nm.

Figure 1 shows a sketch of the probe. A 5 mW, 632 nm He–Ne laser beam was guided through a purged (1 cc/min of N_2) stainless steel sending probe. A CaF_2 window (Oriel Corp., Model 43371, constant transmittance = 0.9 in 200–7000 nm) was mounted on one end. The receiving probe was a replica of the sending probe and had an identical nitrogen purge. The separation distance between the probes represents the measurement length "L". The receiving probe ends in a light-tight enclosure containing the focussing lenses, optical line filters and detectors.

The optical signal from the receiving probe was divided into five parts using several beam splitters. A laser power meter (Newport Corp., Model 982) was used to monitor the absorption line (632 ± 5 nm). Emission signals at 900 ± 50 nm and 1000 ± 50 nm were monitored using two photomultiplier tubes (Hamamatsu, R316). The emission signals at 4000 ± 100 nm and 4500 ± 100 nm were monitored using two PbSe detectors. In previous work (Sivathanu *et al.*, 1991), narrow band width interference filters were utilized. With the requirements of the two additional lines involving infrared beam splitters, the spectral width of the interference filters had to be increased to 50 nm for the 900 and 1000 nm detectors and 100 nm for the 4000 and 4500 nm detectors in order to obtain reasonable signal to noise ratios (SNR). This complicates the data processing as discussed in the following. The resulting SNR for the 900 and 1000 nm channels were greater than 100 while those for the 4500 nm channel were greater than 50. The 4000 nm channel had a limiting SNR of approximately 10.

The outputs of all five detectors were preamplified. The signals from the preamplifiers for the 632 nm, 4000 nm, and 4500 nm detectors were amplified further using lock in amplifiers (Stanford Research, SR510). The frequency response of the three lock in amplifiers was extended to 2000 Hz by modifying their output circuits. The signals at the output of the lock in amplifiers and the PMT preamplifiers were processed through eighth order Butterworth low pass filters (Ithaco, model 3200) operated at 1000 Hz with or without a gain of 10 depending on the signal strength. All five channels of data were sampled at 1000 Hz by an A/D converter and stored in a laboratory computer for processing using the procedure described in the following.

Principle of Operation

Absorption soot volume fractions were found from the measurements of transmittance at 632.8 nm using the Rayleigh limit for small particles. Past multiline measurements (Gore and Faeth, 1988) have suggested that this approximation is adequate for the present flames. Following Tien and Lee (1982), the absorption soot volume fraction was calculated as:

$$f_{va} = -\ln (I_z/I_z^0)\lambda/K_z L. \tag{1}$$

The argument of the natural log in Eq. (1) is the measured transmittance. "L" is the separation distance between the probes. The constant K_z in Eq. (1) involves the complex refractive index of the soot particles ($n - ik$) at the measurement wavelength (Tien and Lee, 1982):

$$K_z = \frac{36\pi nk}{(n^2 - k^2 + 2)^2 + 4n^2k^2}. \tag{2}$$

The complex refractive index of soot particles has been measured by several investigators and considerable discussion of the effects of temperature, fuel type and wavelength exists in the current literature (see for example: Sivathanu *et al.*, 1990, 1991). Consistent with earlier work (Gore and Faeth, 1988; Sivathanu *et al.*, 1990, 1991), the values given by Dalzell and Sarofim (1969) were used resulting in $K_z = 4.89$ at a wavelength of 632 nm.

The interference filter associated with the emission detectors have a relatively large spectral width requiring the use of integration over the filter transmittance curve. The

intensities measured by the emission detectors are related to the local properties as:

$$I_\lambda = \frac{\int_{\lambda_1}^{\lambda_2} (1 - \tau_\lambda) F_\lambda I_{b\lambda} d\lambda}{\int_{\lambda_1}^{\lambda_2} F_\lambda d\lambda}, \tag{3}$$

where τ_λ is the monochromatic transmittance of the material in the probe volume over the probe length L, F_λ is the characteristic transmittance curve of the interference filter with lower and upper cutoff wavelengths of λ_1 and λ_2. $I_{b\lambda}$ is Planck's function at the probe volume temperature T:

$$I_{b\lambda} = \frac{2hc^2}{\lambda^5 (\exp (hc/\lambda k_B T) - 1)}. \tag{4}$$

For the emission measurements at 900, 1000 and 4000 nm, the soot particles in the probe volumes are the dominant contributors to the emission intensity and hence τ_λ. Therefore for these three wavelengths the transmittance in Eqs. (3) is equated to the transmittance due to soot particles:

$$\tau_{\lambda s} = \exp \left(- \frac{K_\lambda f_{ve} L}{\lambda} \right) \tag{5}$$

Where $K_\lambda = 5.33$ for $\lambda = 900$ nm and $K_\lambda = 5.59$ for $\lambda = 1000$ nm are constants dependent on the refractive index of soot (Tien and Lee, 1982). Since h, c and k_B are fundamental constants and K_λ for $\lambda = 900$ nm and $\lambda = 1000$ nm are known, Eqs. (3)–(5) for these two wavelengths were solved for the two unknowns–temperature T and emission soot volume fraction f_{ve}. Due to the integral nature of Eqs. (3), an iterative solution must be obtained. The intensity at 4000 nm originates from soot particles alone and that at 4500 nm originates from soot particles and CO_2 molecules in the probe volume. The temperature and the soot volume fraction are known from the procedure described above. However, there is considerable uncertainty concerning the refractive index of soot and its temperature dependence particularly for wavelengths greater than 2500 nm (Habib and Vervisch, 1988). Therefore, the K_λ for $\lambda = 4000$ nm was treated as an unknown. Equations (3)–(5) were used to obtain this value *in situ*. The K_λ for soot at 4500 nm was equated to that at 4000 nm since the two wavelengths are relatively close.

The transmittance at 4500 nm can be written as:

$$\tau_{\lambda = 4500\,\text{nm}} = \tau_{\lambda s} \tau_{\lambda CO_2}, \tag{6}$$

where $\tau_{\lambda s}$ is given by Eq. (5) and $\tau_{\lambda CO_2}$ is related to the concentration of CO_2, temperature and a collision broadening parameter (Ludwig *et al.*, 1973):

$$\tau_{\lambda CO_2} = \exp (-X^*(1 - Y^{-1/2})^{1/2}), \tag{7}$$

where X^* is the optical depth in the weak line limit:

$$X^* = K_B X_{CO_2} \frac{273}{T} L, \tag{8}$$

where X_{CO_2} is the mole fraction of CO_2 and K_L is a molecular line constant given by Ludwig *et al.* (1973). Y is the combined Doppler and collision broadened line width which is a complicated transcendental function of X_{CO_2}, T, L and concentrations of collision broadening species (assumed to be N_2 in the present). It is not practical to use a root-finding procedure for obtaining the concentration of CO_2 from Eqs. (3), (6)–(8). Therefore, a table of intensity as a function of CO_2 concentration and temperature was developed. the concentration of CO_2 was obtained by linear interpolation in this table. the uncertainty of this procedure was tested using the preliminary tests described later in the article.

It is noted that the emission intensities measured at 900, 1000, 4000 and 4500 nm provide a unique solution for the four unknowns: temperature, emission soot volume fraction, extinction coefficient of soot particles at 4000 nm and CO_2 concentrations. All of these quantities are defined by Eqs. (3)–(8) as effective emission properties for the probe volume. If the probe volume is inhomogeneous, these properties represent a weighted average over the radiation path. Equations (3)–(8) are solved using an iterative procedure. Convergence criteria for the procedure were established as 5 K for the temperature, 0.1 ppm for the soot volume fractions, 10% for the CO_2 mole fractions and 5% for the extinction coefficient of soot particles at 4000 nm. These are within the uncertainties of the present measurement technique as discussed in the following.

Measurement procedures somewhat similar to the one described above have been applied to laminar methane/air flames by Hommert *et al.* (1977) and to dust explosions by Cashdollar and Hertzberg (1982). Hommert *et al.* (1977) measured path integrated CO_2 intensity across a laminar Wolfhard Parker flame and used thermocouple measurements of temperature and a polynomial curve for CO_2 distribution across the flame to deconvolute the data. Negligible interference from soot particles was encountered. It is difficult to apply the deconvolution procedure to turbulent flows for obtaining time dependent data. It is not possible to apply this procedure to optically thick flames studied here.

Cashdollar and Hertzberg (1982) have applied three wavelength and six wavelength emission measurements to the detection of gas and particle temperatures in dust explosions. The limitation of their procedure is that the radiation path must be optically thick for both particles and gas wavelengths. The interference by particles at the gas wavelengths also made these measurements somewhat ambiguous.

The absolute uncertainties in the present measurements depend on the different estimates of refractice indices available in the literature. Following estimates of uncertainties are for a fixed set of refractive indices. It is noted that the effects of the choice of refractive index on f_{va} and f_{ve} are higher than those on the temperature. The uncertainties in the temperature measurements were less than 40 K for $f_{ve} > 0.1$ ppm increasing to about 80 K for $f_{ve} = 0.01$ ppm. Crosschecks of results with three different wavelengths (514 nm, 800 nm and 2300 nm) as well as repeated measurements were used to confirm the above uncertainty. The uncertainties in the absorption soot volume fractions were less than 10% at 10 ppm increasing to approximately 40% at 0.01 ppm due to digitization errors. The uncertainties in the emission soot volume fraction measurements are dominated by the uncertainties in the measurement of temperatures using Eq. (3). The uncertainties in the emission soot volume fraction measurements are less than 25% at a temperature of 1400 K and f_{ve} of 1 ppm. Assuming that the effective radiation temperatures of soot particles and CO_2 over the probe volume are identical, the uncertainty in the CO_2 concentration measurements are estimated to be less than 25% based on repeated measurements and also tests using a premixed methane/air flat flame burner described later in the article. The

uncertainty introduced by possible difference in the effective temperature of soot and CO_2 in the probe volume is presently unknown. It is noted that Pagin and Okoh (1984) have shown that when soot particles and the gases surrounding them are well mixed, their temperatures are identical within a few Kelvin. The temperature differences between gas and soot in the present case may exist only because of the inhomogeneous distributions within the probe volume. These difficulties could be resolved by conducting measurements at additional CO_2 wavelengths.

Resolved Length Scales

Measurements of length scales of turbulent fluctuations in the present strongly radiating flames are not currently available. However, the interpretation of the present data depends heavily on information concerning turbulent length scales relevant to radiation properties. Therefore, these scales are estimated from existing data concerning nonluminous flames (Kounalakis *et al.*, 1991).

Kounalakis *et al.* (1991) have measured statistical properties of two point correlations of mixture fractions in nonluminous turbulent jet flames for jet exit Reynolds numbers of 7400 and 12700. The integral scales of mixture fraction fluctuations using Mie scattering from solid particle seed were reported to be $0.016x$ where x is the axial distance from the injector exit. The scales were found to be independent of radial position and also relatively independent of Reynolds number. Kounalakis *et al.* (1991) have also found that the estimates of scales based on their Mie scattering experiments are approximately 50% lower than those for the gas phase processes due to negligible diffusivity of the solid particles. Thus, $0.032x$ is an appropriate estimate of the integral length scales of mixture fraction fluctuations in their flames. If it is assumed that the hydrodynamics of the mixing process in the nonluminous and luminous flames are similar then the present probe is capable of resolving the integral scales of mixture fraction flucutations at axial positions beyond approximately $x/d = 30$. Therefore, two measurements locations ($x/d = 30$ and $x/d = 50$) were selected for the present measurements.

Resolution at the integral scale of turbulent mixing was found adequate by Kounalakis *et al.* (1991) for the prediction of mean and statistical properties of radiation intensity from nonluminous flames. Sivathanu *et al.* (1991) predicted mean and statistical properties of raidation intensity from the present turbulent flames using the spatial resolution of the present probe. However, the variation of temperature and soot volume fraction within an integral scale sized eddy had to be treated via the use of the emission soot volume fraction and the two line temperature in order to obtain reasonable predictions. Conceptually, this problem is similar to the one encountered in numerical simulations of turbulent flows where the smallest practically resolvable scale is not adequate to describe the process and appropriate subgrid scale models are essential. The probe volume of the present measurements defines the smallest resolvable scale which is estimated to be as large as the integral scale of mixing. The subgrid scale structure results from the presence of soot in approximately 1 mm thick streaks first observed by Gore and Faeth (1988). Gore and Jang (1990) have found that these streaks result in significant temperature inhomogeneity within the probe volume due to radiative cooling. Thus, the soot and radiation process alter the length scales over which temperatures vary. However, whether it is necessary to resolve these subgrid scale effects in a transient manner is unknown. The present results combined with those of Sivathanu *et al.* (1991) are expected to clarify this issue further. It is noted that the thin soot streaks are formed as a result of soot formation and oxidation

processes and do not broaden to the mixing scales due to negligible diffusivity (Schmidt number effect) of soot.

Data Collection and Processing

After establishing a steady flame, the five detector signals were monitored using a LABPAC A/D converter and a laboratory computer. The sampling frequency per channel was set at 1000 Hz and a total of 6000 points per channel were collected from each run (6 s steady flame operation time). The flame was then shut off and the data stored in files. The background readings were obtained and stored (approximately 20 seconds after the flame data). The test was repeated 2 times at each location providing as many 6 s realizations of the five signals. It was found that the resulting 12 s records of the data were adequate for obtaining converged (within the present experimental uncertainties) estimates of mean and RMS properties. Six locations (at radial positions of $r/x = 0$, 0.04 and 0.08 at axial positions of $x/d = 30$ and 50) were selected to obtain statistical information concerning T, f_{ve} and X_{CO_2}. At these locations, the tests were repeated 10 times to collect a 60 s record of the data. The 60 s records were found adequate for obtaining converged estimates of various conditioned and unconditioned probability distribution functions (PDFs).

In the intermittent region near the edge, the laser absorption and emission (especially at 900 nm and 4000 nm) frequently were below the detection limits of the present instrument. In such cases, the temperature was assumed to be 300 K, the soot volume fraction and the carbon dioxide mole fraction were assumed to be 0. These assumptions lead to a bias in the downward direction for all data. The bias in the soot volume fractions was below 0.1 ppm. The estimated bias in the mean temperatures near the edge was 150 K and the estimated bias in the CO_2 concentrations near the edge was 0.02. From the entire data, the lower detection limits of the instrument were determined to be 900 K for temperature, 0.1 PPM for absorption soot volume fractions, 0.1 PPM at 1400 K for emission soot volume fraction and 0.05 for the mole fraction of CO_2. Values of these variables below these values are not separable from the background. However, these values do not contribute significantly to radiation heat transfer.

Preliminary Tests

The purpose of the preliminary tests was to evaluate the present tables for obtaining X_{CO_2}. This was accomplished using a hot combustion gas generator described by Gore *et al.* (1990) and Meng (1990). The hot gas generator involves flat premixed flames burning metered methane/air mixtures stabilized over porous ceramic disks. The post flame gases pass through an air dilution chamber. The diluted mixture passes through a contoured ceramic nozzle of 12.5 mm exit diameter. The nozzle contour leads to uniform velocity, composition of major species and temperature over 90% of the exit area with low (less than 5%) turbulence intensity. The concentration of CO_2 in the exhaust gases is measured using isokinetic sampling and analysis using an online gas analyzer (Beckman Industries, model No. 864). The gas analysis equipment was calibrated before and after each run with zero and calibration gases. The temperature of the gas stream was measured using fine wire thermocouples (Pt – Pt + Rh13%) and corrected for radiation losses. The maximum uncertainties in the gas concentration measurements are estimated to be 10% while those in the temperature measurements are estimed to be 50 K. These inherent uncertainties in the present test equipment affect the results of the tests. The five line emission/absorption probe was

TABLE I
Results of the CO_2 concentration check.

X_{CO_2} Calib.	T, K	X_{CO_2} Measured	Error %
6.1	1200	7.6	+24.5
7.0	1350	5.8	−17
7.7	1510	7.4	−4
8.4	1696	7.5	−11
8.0	1628	7.6	−5
7.8	1215	7.2	−8

inserted at 20 mm from the exit plane of the ceramic nozzle. Naturally, for the fuel lean premixed flames, only the 4500 nm channel provided a measurable signal. This test allowed an examination of the zero readings on the three emission channels and also of the effects of probe heat up. Table I shows the results of the tests for CO_2 concentration measurements. The error in the worst case is approximately 25% but generally lower than this value.

The above test apparatus was also used for studying the effects of probe disturbances and quenching on the properties of the material passing through the probe volume. The perturbations in the properties of the flames caused by the introduction of the probes were evaluated by comparing measurements of mean CO_2 concentrations with and without the probes. Maximum error in the mean concentrations due to the presence of optical probes were less than 5% (of the mean concentration) which is within the uncertainty. Effects of probes on the local temperatures were also evaluated using thermocouple measurements with and without the optical probes. The effect of optical probes on the local temperatures was less than 5 K. Additional tests to examine the perturbations introduced by the probes involved changing the separation distance by a factor of 2. The results of this examination showed that the probe perturbations on the quantities of interest are less than 2% for separation distances greater than 5 mm. Additional sources of errors due to the present intrusive probes arise from the buildup of soot particles on the probe surfaces and from heating up of the tubes. These errors were controlled by limiting the test times to less than 40 seconds. The maximum errors in the intensity data caused by probe heat up were less than 1% which is well within other uncertainties.

Operating Conditions and Measurement Locations

Measurements were completed for two different burner exit Reynolds numbers (Re = 5300 and Re = 9200) calculated based on the burner diameter and the cold gas properties. The operating conditions were identical to the flames studied by Gore *et al.* (1989) and Sivathanu *et al.* (1991). The burner exit Reynolds numbers were also identical to those of the two flames studied by Gore and Faeth (1988). These operating conditions were selected in order to take advantage of the large amount of existing data concerning the flames. Table II summarizes the operating conditions. The flow rates of fuel were monitored using a calibrated rotameter. The heat release rates were estimated using ideal heat of combustion. The flows were turbulent and momentum dominated at the jet exit but the downstream locations were significantly influenced by buoyancy.

TABLE II
Summary of operating conditions.

Re	m mg/s	*Q* (kW)
5300	271	13.05
9200	470	22.6

Path Integrated Radiation Intensity Measurements

In order to test the analysis described in the following section, measurements of radiation intensity were completed for various radiation paths at an axial location of $x/d = 50$ within the flames. The radiation paths were symmetric around the flame axis and were progressively increased in length thus including locations farther away from the axis. This was accomplished by mounting the purged probes on two horizontal traverses. The traverses shown by arrows on Figure 1 control the distance between the two probes as shown. After each movement of the probes, the alignment was checked using the He–Ne laser beam. The changes in the view angle for different separation distances were accounted for by obtaining a separate black body calibration for each position. The data were processed to obtain mean and root mean square monochromatic radiation intensities at all the emission wavelengths. These data were used to evaluate a multivariate stochastic analysis described in the following.

Sivathanu *et al.* (1991) reported the measurements and predictions of the monochromatic radiation intensity using a bivariate analysis for $\lambda = 900$ and 1000 nm. Sivathanu and Gore (1990) verified the analysis for $\lambda = 2300$ nm. This procedure allows an evaluation of each term in the summation represented by the equation of radiative transfer. In the present study, the measurements and predictions for the soot radiation intensity at $\lambda = 4000$ nm and the combined CO_2 and soot radiation intensity at $\lambda = 4500$ nm were compared.

Multivariate Stochastic Analysis

A single variable (mixture fraction) has been simulated using stochastic time series analyses by Kounalakis *et al.* (1991). Sivathanu *et al.* (1990) simulated soot volume fractions and underfire–overfire intermittency using two time series. However, a cross correlation between the two variates was not established. The simulation of soot absorption coefficient in conjunction with the two level temperature model resulted in an unknown positive (in contrast to the experimental data) cross correlation between temperature and soot volume fractions. Sivathanu *et al.* (1991) completed a bivariate (soot volume fraction and temperature) stochastic analysis to account for the strong effects of cross correlations between these variables. In the following, the results of this analysis are summarized and the method for extending it to multivariate analysis (trivariate in the present case) is briefly summarized.

The fluctuation in soot volume fraction around its mean value was simulated as an independent variate, using a first order auto-regressive scheme, Box and Jenkins (1976), similar to earlier analyses:

$$f_v'(t + \Delta t) = \Phi_{f_v} f_v'(t) + a_{f_v}(t + \Delta t), \tag{9}$$

where Φ_{f_v} is the auto-correlation coefficient of soot volume fraction. a_{f_v} is a random shock with zero mean chosen to satisfy the required probability density function of f_v, *i.e.*,

$$\overline{a_{f_v}^2} = \overline{f_v'^2}(1 - \Phi_{f_v}^2). \tag{10}$$

The time series for temperature was simulated as a first-order ARIMA (Auto-Regressive Integrated Moving Average) process, Box and Jenkins (1976), which can be represented as follows:

$$T'(t + \Delta t) = \Phi_T T'(t) + \Phi_{f_v T} a_{f_v}(t + \Delta t) + a_T(t + \Delta t), \tag{11}$$

where Φ_T is the auto-correlation coefficient of T. $\Phi_{f_v T}$ is the moving average part chosen to satisfy the cross-correlation between soot volume fraction and temperature and a_T is the random shock chosen to satisfy the PDF of temperature. $\Phi_{f_v T}$ is given by:

$$\Phi_{f_v T} = \overline{f_v' T'}(1 - \Phi_T \Phi_{f_v})/\overline{a_{f_v}^2}, \tag{12}$$

and $\overline{a_T^2}$ is given by:

$$\overline{a_T^2} = \overline{T'^2}(1 - \Phi_T^2) - \Phi_{f_v T}^2 \overline{a_{f_v}^2}. \tag{13}$$

In the present study, this procedure was extended to include a time series for X'_{CO_2} that includes its cross correlations with temperature and soot volume fractions. Although the equations are somewhat lengthier than Eqs. (9)–(13), the procedure is identical and the resulting equations are not listed here.

With the variables f_v', T and X'_{CO_2} obtained from the trivariate time series analysis, the instantaneous radiation intensity was calculated using the RADCAL algorithm of Grosshandler (1980). This series can be treated as stochastic data to obtain mean and RMS intensities for comparison with data. To avoid the uncertainty of using an analytical PDF, a PDF consisting of discrete data was used. The statistical properties of this time series were also obtained and compared with experimental data. In the present paper, the results for the mean radiation intensities are discussed as a first step. It is noted that due to the nonlinear dependence of radiation intensities on scalar properties, stochastic analysis described above is necessary for the prediction of mean radiation intensity.

As discussed before, the present data are resolved to the integral scale of mixing based on the work of Kounalakis *et al.* (1991). Therefore, treatment of spatial correlations is not necessary in the time series analysis. However, as discussed above, Sivathanu *et al.* (1991) found that an appropriate subgrid scale model involving use of the emission soot volume fractions and two line temperatures is necessary for accurate prediction of radiation intensity. In this work, the treatment was extended to include intensities at 4000 nm from soot and intensities at 4500 nm from soot and CO_2.

RESULTS AND DISCUSSION

The discussion of the present results is facilitated by considering the variation of species concentration and soot volume fractions as a function of fuel equivalence ratio (which is a single valued function of mixture fraction) measured by Gore and Faeth (1988) using laminar diffusion flames. According to these measurements, concentrations of CO_2 reaches 5% approximately at equivalence ratios of 0.3 and 6. Under the laminar flamelet approximation, this establishes the range of equivalence ratios where meaningful data can be obtained using the present instrument. The graph of soot

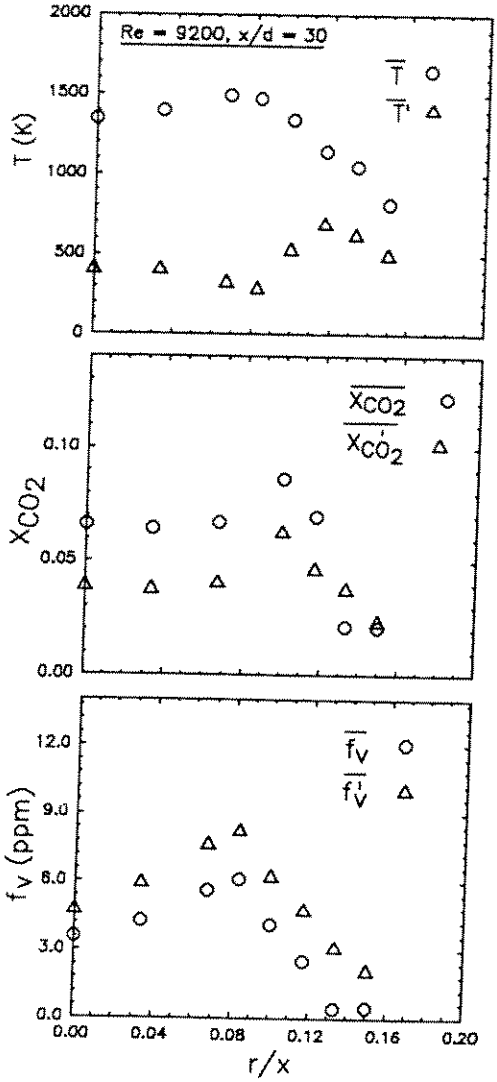

FIGURE 2 Radial profiles of mean and RMS scalar properties, $x/d = 30$, $Re = 9200$.

volume fractions from Gore and Faeth (1988) shows that this range covers all of the soot profiles reasonably well. Outside the measuring range, the CO_2 concentrations and soot volume fractions are set to 0 and the temperature is set to 300 K by the present procedure. The procedure down-biases the average somewhat. But since the interest is in radiation heat transfer, the erors outside the range covered by the present measurements are insignificant.

Measurements of mean quantities are discussed first. Figure 2 shows distributions of temperature, CO_2 concentrations and soot volume fractions based on emission, f_{ve}, plotted as a function of normalized radial distance for $x/d = 30$. Sivathanu *et al.* (1991) have found that the soot volume fractions based on absorption, f_{va}, are larger by factors of up to 7 compared to those based on emission. Since emission soot

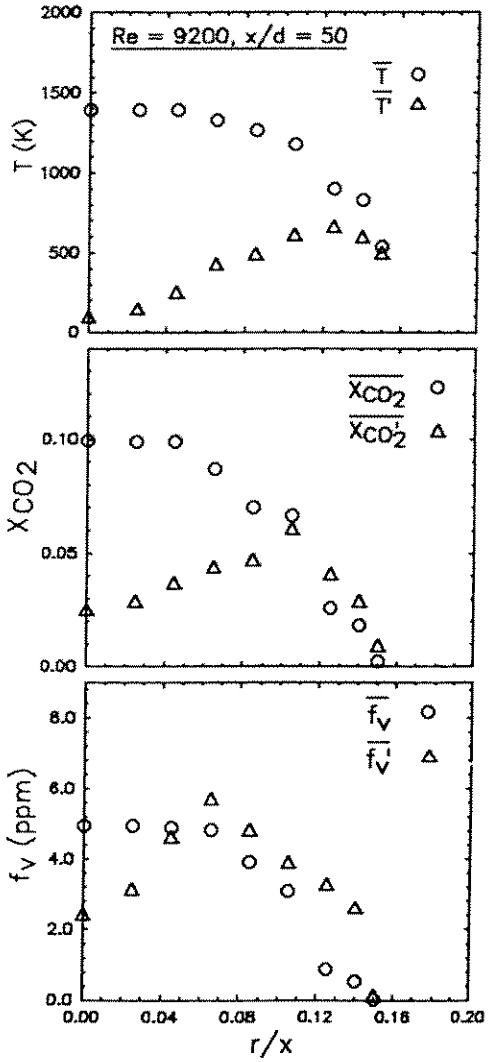

FIGURE 3 Radial profiles of mean and RMS scalar properties, $x/d = 50$, $Re = 9200$.

volume fractions contribute to the radiation heat flux, these are considered in the present paper. The temperature is around 1350 K at the centerline and then increases to approximately 1550 K as the flame sheet is approached. The RMS fluctuations in temperature are approximately 400 K near the axis and decrease as the temperature peak is approached as expected. The turbulence intensity of temperature fluctuations is thus approximately 25% near the axis. Near the edge the measured mean temperatures decrease and the temperature fluctuations increase due to intermittency and due to fuel lean conditions. The mean CO_2 concentrations are lowest at the center as expected for fuel rich conditions. The concentrations increase as the flame sheet is approached as expected. The fluctuations in the CO_2 concentrations are almost 50% of the mean at the center decrease near the peak CO_2 concentration region. The mean

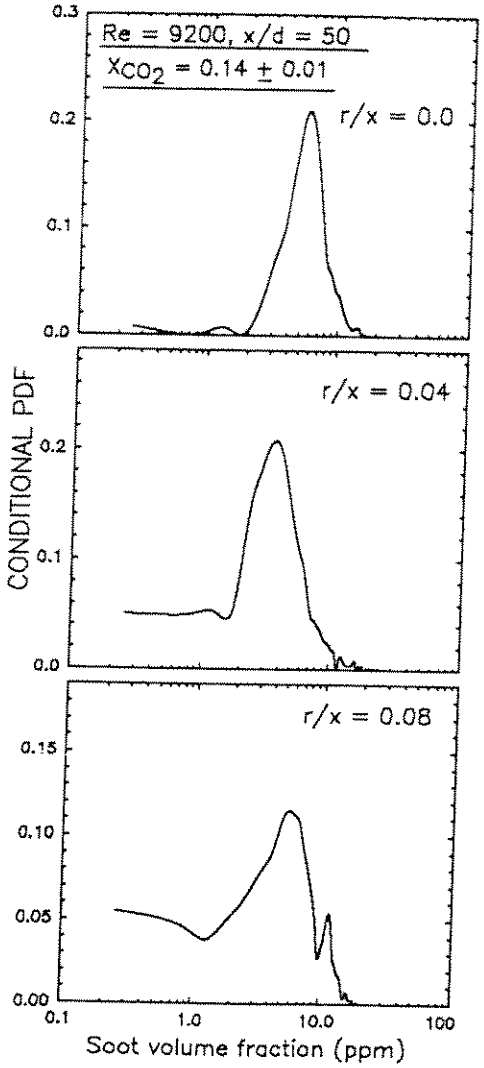

FIGURE 4 Conditional PDF of soot volume fractions, $X_{CO_2} = 0.14$.

CO_2 concentrations are almost constant near the middle third of the flame. The soot volume fractions increase as the flame sheet is approached and peak at a location just on the fuel rich side of the peak CO_2 concentrations. Soot volume fractions show very high fluctuation intensities (up to 90%).

Figure 3 shows the radial distributions of T, X_{CO_2} and f_{sv} for $x/d = 50$ representing longer time for radiative cooling. As expected the mean temperature profile is much flatter and the turbulence intensity has decreased. The CO_2 profile shows higher value near the center for this downstream location. The fluctuation intensity of CO_2 has decreased substantially from its value at $x/d = 30$. The reasons for this behavior are presently being investigated. The mean f_{sv} are lower than those at $x/d = 30$ while the RMS f_{sv} are similar to those at $x/d = 30$.

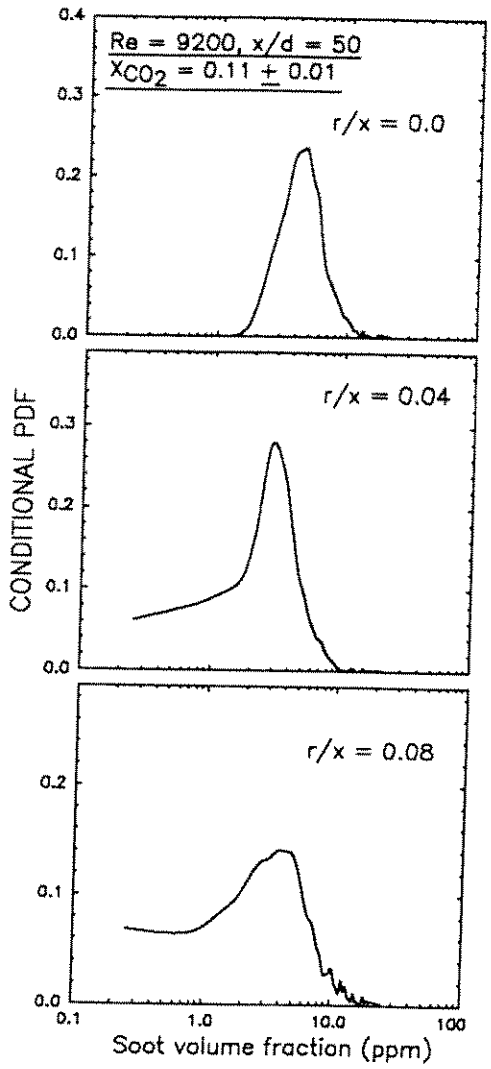

FIGURE 5 Conditional PDF of soot volume fractions, $X_{CO_2} = 0.11$.

The transient measurements yielded by the present probe are studied using conditional probability density functions in the following. Figure 4 shows the conditional PDF of f_{ve} at $x/d = 50$ for three radial positions. The conditioning is performed with respect to a X_{CO_2} bin of 0.14 ± 0.01. Based on the data of Gore and Faeth (1988), this corresponds to an equivalence ratio range of 0.9–1.0 on the fuel lean side and 1.0–1.2 on the fuel rich side. Thus the material in the probe volume represents flame sheet conditions within the uncertainty of the present data. Based on the distribution of soot in the laminar flames shown by Gore and Faeth (1988), it appears that the high soot conditions would mark the fuel rich points and vice versa. The conditional PDF at the axis shows this behavior since there is almost zero probability of finding f_{ve} values less than 1 PPM. As we progress radially outward, samples from the lean

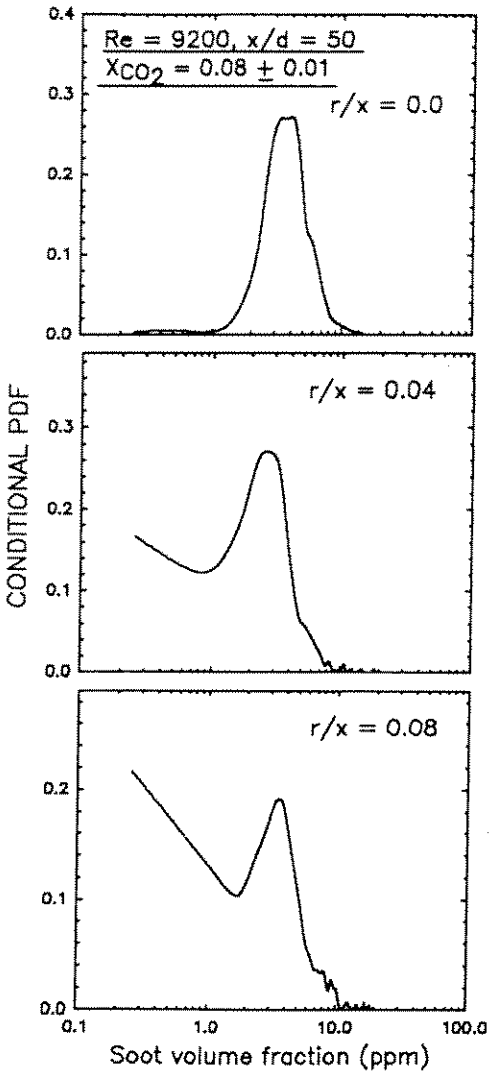

FIGURE 6 Conditional PDF of soot volume fractions, $X_{CO_2} = 0.08$.

conditions are obtained as well and the probability of finding f_{ve} below 1 PPM increase considerably. A range of values varying over a factor of 10 have almost the same probability perhaps due to the steep variation of soot volume fractions with equivalence ratio seen on the fuel lean side. The probability of finding lean flamelets increases further as $r/x = 0.08$ is considered. The shape of the conditional PDFs from three different positions above $f_{ve} > 1$ PPM shows that the flamelets traversing the probe volume at these three locations have similar structure.

The conditional PDF of f_{ve} for X_{CO_2} bin equal to 0.11 ± 0.01 is shown in Figure 5. The equivalence ratio range covered by this bin is 0.55–0.65 on the lean side and 2.0–2.4 on the fuel rich side. The peak soot volume fractions observed at all three radial locations are almost the same as those seen in Figure 5 for higher CO_2

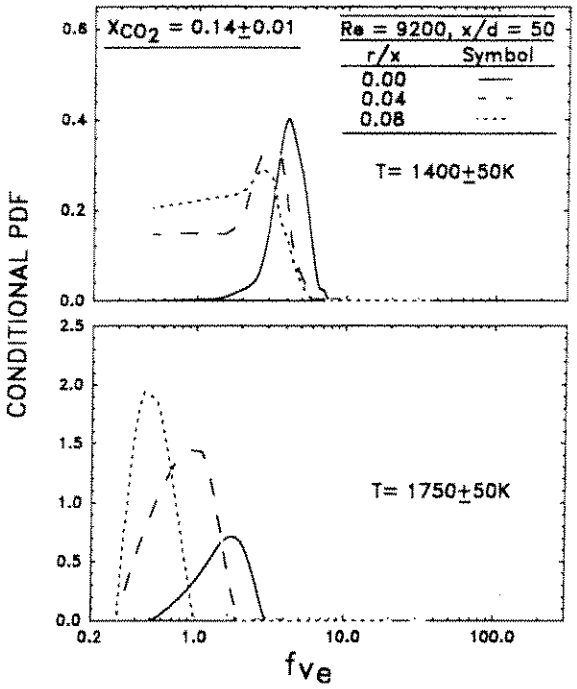

FIGURE 7 Conditional PDF of soot volume fractions, $X_{CO_2} = 0.14$, $T = 1400$ K, $T = 1750$ K.

concentrations. Again, the rich conditions at flame axis are apparent and low f_{ve} are seen only at the positions away from the center. The shapes of the PDFs for $f_{ve} > 1$ PPM at the three radial positions are similar. However, smaller sample size at the $r/x = 0.08$ positions distorts the PDF somewhat. On the fuel lean side almost a factor of 10 variation is again observed. The comparison of the conditional PDFs for the two X_{CO_2} values suggests that the relationship between soot volume fractions and equivalence ratios in turbulent flames also shows behavior similar to that observed by Gore and Faeth (1988), where hydrodynamic effects moved the soot particles (which have very low molecular diffusivity) to fuel rich regions in the lower reaches of the laminar flame and to the fuel lean regions further above. The relatively large uncertainties in the present CO_2 measurements also explain part of the scatter.

The extent of the scatter was studied further by considering conditional PDFs for X_{CO_2} values in the range 0.08 ± 0.01 as shown in Figure 6. The conditional PDFs show similar shapes. As expected the probability of low f_{ve} at the axis is very low and increases progressively as radially outward conditions are considered. The probability of very low soot concentrations increase substantially for the position near the edge due to predominantly fuel lean conditions. Thus the scatter shown by the soot volume fractions-equivalence ratio relationships in the turbulent flames is similar to that in laminar flames observed by Gore and Faeth (1988). Therefore, in the present turbulent flames ($Re = 9200$), negligible laminar diffusivity of soot particles appears to be important in determining its volume fraction. It is noted that a similar conclusion can be reached based on the differences in length scales of mixing and soot volume fractions discussed earlier.

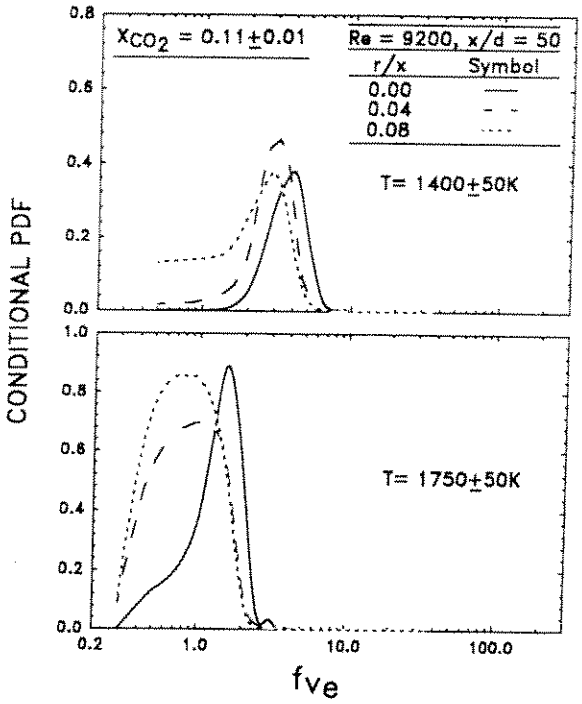

FIGURE 8 Conditional PDF of soot volume fractions, $X_{CO_2} = 0.11$, $T = 1400$ K, $T = 1750$ K.

The present transient measurements allow conditioning of the soot volume fractions into X_{CO_2} bins and temperature bins simultaneously. Thus, the thermodynamic state within the probe volume is well defined within the present subgrid scale model and then the soot volume fractions within the probe volume are studied. Figure 7 shows conditional PDFs of f_{ve} for $X_{CO_2} = 0.14 \pm 0.01$ and $T = 1400 \pm 50$ K as well as $T = 1750 \pm 50$ K. As discussed before the X_{CO_2} bin defines the equivalence ratio to be close to stoichiometric based on the data of Gore and Faeth (1988). Naturally, the temperature differences are caused by variations in the state of radiative cooling. From Figure 7 it is observed that the lower temperature bin implies that f_{ve} is higher particularly at the centerline where slightly fuel rich conditions persist. For the higher temperature bin all of the soot volume fractions are lower. The positions near the edge show larger probability of lower f_{ve} at higher temperatures corresponding to regions resulting from oxidation of soot. The conditional PDFs show an almost exclusive behavior based on temperature bins. Thus if there is large quantity of soot at a location, it must be at low temperature. Since large quantities of soot exist on the slightly fuel-rich side of the flames sheet, these results imply a steep temperature gradient on the fuel rich side as predicted by the transient numerical analysis of Gore and Jang (1990).

Figure 8 shows conditional PDFs of f_{ve} for $X_{CO_2} = 0.11 \pm 0.01$ and $T = 1400 \pm 50$ K as well as for $T = 1750 \pm 50$ K. As before, the lower temperature bin almost exclusively shows high f_{ve} and the higher temperature bin shows the lower f_{ve}. The positions at larger radii and at lower temperatures also show some low f_{ve} values probably corresponding to material that had higher soot loading at some point in time.

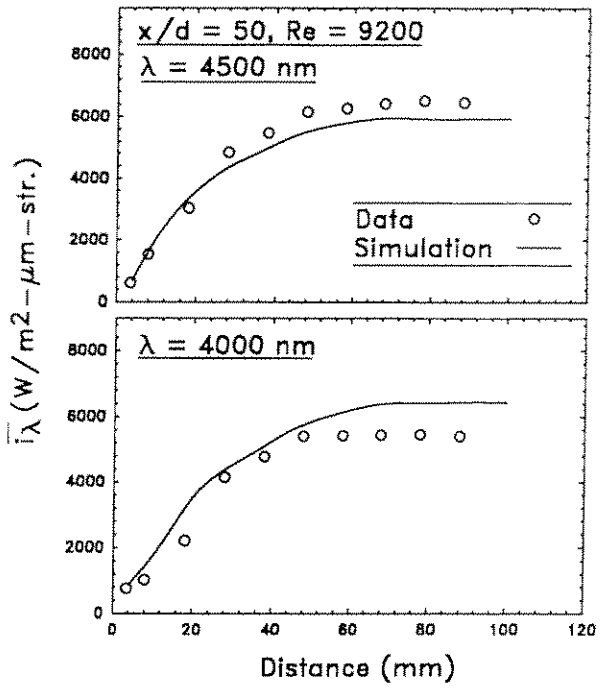

FIGURE 9 Measurements and predictions of radiation intensity at 4000 and 4500 nm.

Monochromatic Radiation Intensity

In order to test the present multivariate analysis, radiation intensities for radiation paths that are symmetric around the axis of the flames were considered as discussed before. Figure 9 shows predictions and measurements of the mean radiation intensity as a function of distance between the probes for $\lambda = 4000$ and $\lambda = 4500$ nm. The intensity at 4000 nm involves radiation from soot particles and that at 4500 nm involves radiation from both CO_2 molecules and soot particles. In both cases the predictions agree reasonably well with the measurements supporting the present approach.

SUMMARY AND CONCLUSIONS

In the present study, the first transient simultaneous measurements of temperatures, soot volume fractions and CO_2 concentrations resolved to the integral length scale of mixing were obtained. Measurements showed that the material within this scale had large temperature and soot volume fraction inhomogeneities. In particular, the soot streaks in the present flames were at substantially lower temperatures than the flame sheet due to the effects of radiative cooling. Whether this inhomogeneity affects the present data must be determined using measurements of effective radiation temperatures of CO_2. A stochastic multivariate procedure resolved to the integral scale was developed and reasonably good predictions of mean and RMS radiation intensities at 4000 nm and 4500 nm were obtained. Combined with previous results for 514, 632, 900, 1000 and 2300 nm, it appears that the present simulation can be used to predict the radiative heat transfer from strongly radiating flames. Theoretical

methods to predict the present subgrid scale quantities- emission soot volume fractions, radiation temperatures, CO_2 concentrations and cross correlations of these quantities need to be developed.

ACKNOWLEDGEMENTS

This study is supported by the National Science Foundation under Grant Number CTS-8914520 with Drs. Charles Garris, Joan Gosink and William Grosshandler serving as NSF Scientific Officers. Instrumentation support provided by the Engineering Research Center, College of Engineering and the Mechanical Engineering Department of the University of Maryland at College Park and Baltimore County is acknowledged.

REFERENCES

Becker, H. A. and Liang, D. (1983). Soot Emission, Thermal Radiation and Laminar Instability of Acetylene Diffusion Flames. *Combust. Flame* **52,** 247–256.

Box, G. E. P. and Jenkins, G. M. (1976). *Time Series Analysis*, Holden Day, San Francisco, CA.

Cashdollar, K. L. and Hertzberg, M. (1982). Infrared Pyrometers for Measuring Dust Explosion Temperatures. *Optical Engineering* **21,** (1) 82–86.

Dalzell, W. H. and Sarofim, A. F. (1969). Optical Constants of Soot and their Application to Heat Flux Calculations. *J. Heat Trans.* **91,** 100–104.

Gore, J. P. and Faeth, G. M. (1988). Structure and Spectral Radiation Properties of Turbulent Acetylene/Air Diffusion Flames. *J. Heat Trans.* **110**(1), 173–181.

Gore, J. P., Ip, U. S., and Sivathanu, Y. R. (1990). Coupled Structure and Radiation Analysis of Acetylene/Air Flames. *J. Heat Trans.*, submitted.

Gore, J. P. and Jang, J. H. (1990). Transient Radiation Properties of a Subgrid Scale Eddy. *Heat and Mass Transfer in Fires and Combustion Systems*. ASME HTD **148**, ASME, New York, pp. 57–64.

Gore, J. P., Meng, W. H., and Jang, J. H. (1990). Droplet Flame Extinction in Combustor Environments. *AIAA paper no. 90-0467*, AIAA, Washington D.C.

Grosshandler, W. L. (1980). Radiative Transfer in Nonhomogeneous Gases: A Simplified Approach. *Int. J. Heat Mass Trans.* **23,** 1447–1457.

Habib, Z. G. and Vervisch, P. (1988). On the Refractive Index of Soot at Flame Temperature. *Combust. Sci. and Tech.* **59,** 261–274.

Hommert, P. J., Viskanta, R., and Mellor, A. M. (1977). Flame Temperature Measurements by Spectral Remote Sensing. *Combust. Flame* **30,** 295–308.

Kent, J. H. and Bastin (1984). Parametric Effects on Sooting in Turbulent Acetylene Diffusion Flames. *Combust. Flame* **56,** 29–42.

Kounalakis, M. E., Sivathanu, Y. R., and Faeth, G. M. (1991). Infrared Radiation Statistics of Nonluminous Turbulent Diffusion Flames. *Proceedings of the ASME/JSME Thermal Engineering Joint Conference 1991*, **5,** ASME, New York, pp. 3–12; also *J. Heat Trans.*, submitted.

Ludwig, C. B., Malkmus, W., Reardon, J. E., and Thomson, J. A. (1973). *Handbook of Infrared Radiation from Combustion Gases*, NASA SP-3080.

Magnussen, B. F. (1975). An Investigation into the Behavior of Soot in a Turbulent Free Jet C_2H_2-Flame. *Fifteenth Symposium (International) on Combustion*. The Combustion Institute, Pittsburgh, pp. 1415–1425.

Meng, W. H. (1990). A Study of Droplet Flames in Reactive Environments. Ph.D. Thesis, University of Maryland, College Park, MD.

Pagni, P. J. and Okoh, C. I. (1984). Soot Generation Within Radiating Diffusion Flames. *Twentieth Symposium (International) on Combustion*. The Combustion Institute, Pittsburgh, PA, pp. 1045–1054.

Sivathanu, Y. R., Kounalakis, M. E., and Faeth, G. M. (1990). Soot and Continuum Radiation Statistics of Luminous Turbulent Diffusion Flames. *Twenty-Third Symposium (International) on Combustion*, The Combustion Institute, Pittsburgh, PA, in press.

Sivathanu, Y. R. (1990). *Soot and Radiation Properties of Buoyant Turbulent Diffusion Flames*, Ph. D. Thesis, The University of Michigan, Ann Arbor, MI.

Sivathanu, Y. R., Gore, J. P., and Dolinar, J. (1991). Transient Temperature and Soot Volume Fractions in Strongly Radiating Flames. *Comb. Sci. Tech.* **76,** (1–3), 45–67.

Sivathanu, Y. R. and Gore, J. P. (1990). Transient Scalar Properties of Luminous Pool Flames. *Proceedings of the Fall Technical Meeting of the Eastern States Section on the Combustion Institute*. The Combustion Institute, Pittsburgh, PA, pp. 57.1–57.4. Tien, C. L. and Lee, S. C. (1982). Flame Radiation. *Prog. Energy Combust. Sci.* **8,** 41–59.